Coarse graining the dynamics of nano-confined solutes: the case of ions in clays

Antoine Carof, Virginie Marry, Mathieu Salanne, Jean-Pierre Hansen, Pierre Turq, Benjamin Rotenberg

RESEARCH ARTICLE

Coarse-graining the dynamics of nano-confined solutes: The case of ions in clays

Antoine Carof[a], Virginie Marry[a], Mathieu Salanne[a], Jean-Pierre Hansen[a], Pierre Turq[a] and Benjamin Rotenberg[a]*

[a] *CNRS and UPMC Univ-Paris06, UMR 7195, PECSA, F-75005, Paris, France*
(*Received 00 Month 200x; final version received 00 Month 200x*)

We investigate the possibility of describing by a continuous solvent model the dynamics of solutes confined down to the molecular scale. We derive a Generalized Langevin Equation (GLE) for the generic motion of a solute in an external potential using the Mori-Zwanzig formalism. We then compute the corresponding memory function from molecular simulations, in the case of cesium ions confined in the interlayer porosity of montmorillonite clays, with a very low water content (only six solvent molecules per ion). Previous attempts to describe the dynamics of cesium in this system by a simple Langevin equation were unsuccessful. The purpose of the present work is not to perform GLE simulations using the memory function from molecular simulations, but rather to analyze the separation of time scales between the confined ions and solvent. We show that such a separation is not achieved and discuss the relative contribution of the ion-surface, ion-solvent and ion-ion interactions to the dynamics. On the ps time scale, the ion oscillates in a surface-and-solvent cage, which relaxes on much longer time scales extending to several nanoseconds. The resulting overall dynamics ressembles that of glasses or diffusion inside a solid by site-to-site hopping.

Keywords: Generalized Langevin Dynamics, confinement, memory function, clays, cesium

1 Introduction

The dynamics of confined fluids differs dramatically from their bulk counterparts, especially when the length scale of the confinement becomes comparable to the molecular size [1]. In such cases, the hydrodynamic flows may depart from the predictions of continuous theories, even when modified boundary conditions at the wall are introduced, because of the layering due to the finite size of the fluid molecules [2]. Under even more extreme confinement, where one or two molecular layers of fluid are present, hydrodynamic descriptions are not relevant anymore. While molecular simulation remains the reference theoretical tool to investigate such situations, resort to continuous models is obviously necessary if one wishes to understand the evolution of large systems over long time scales. For example, diffusion models may still be relevant, since the motion of fluid molecules on very long time scales remains diffusive. Nevertheless such models may not accurately reflect the underlying microscopic mechanism, which may differ significantly from that for bulk diffusion. In particular, while the Brownian theory of diffusion, which relies on a separation of time scales between the solute and its surrounding medium is expected to break down [3, 4].

As an example of extremely confined solute, we investigate the case of cesium ions confined in the interlayer porosity of montmorillonite clays, with a very low water content (a single water layer with 6 water molecules per ion), for which previous attempts to build a continuous solvent

*Corresponding author. Email: benjamin.rotenberg@upmc.fr

model failed to reproduce the dynamics predicted by molecular simulations [5, 6]. We first derive a Generalized Langevin Equation (GLE) for the motion of a solute in an external potential using the Mori-Zwanzig formalism. We then compute the corresponding memory function from molecular simulations. The purpose of the present work is not to perform GLE simulations using this memory kernel, but rather to investigate its properties. In particular, we discuss the separation of time scales between the confined ions and solvent. We show that such a separation is not achieved and analyze the relative contribution of the ion-surface, ion-solvent and ion-ion interactions to the dynamics. This explains why the dynamics of this ion under extreme confinement cannot be described by a simple Langevin equation, as was previously attempted.

2 Theory: from Newtonian to Langevin and Generalized Langevin dynamics

2.1 *Continuous solvent model for ions confined in clay interlayers*

We consider here the case of ions confined in the interlayer porosity of clay minerals. These layered aluminosilicate minerals are abundant in the Earth's crust and play an important role in many environmental and industrial processes. Their low porosity and their surface charge control the mobility of ions through their multi-scale porosities and the sorption of these ions on the various types of surfaces they offer. This in turn explains their consideration *e.g.* for the retention of toxic and radioactive waste. Experimental evidence suggests that in clay rocks the major pathways for cations is the so-called interlayer porosity [7], where the counter-ions compensate the negative charged of the mineral layers (see Figure 1). The interlayer space may also contain some water, in quantities which depend among other on the surface charge density and the nature of the counter-ion. In particular, for montmorillonite clays with cesium counterions at low relative humidity (and/or high confining pressure), the most stable state corresponds to a water monolayer, with only ≈ 6 water molecules per cation. The distance between the confining surfaces is then comparable to the molecular and ionic size.

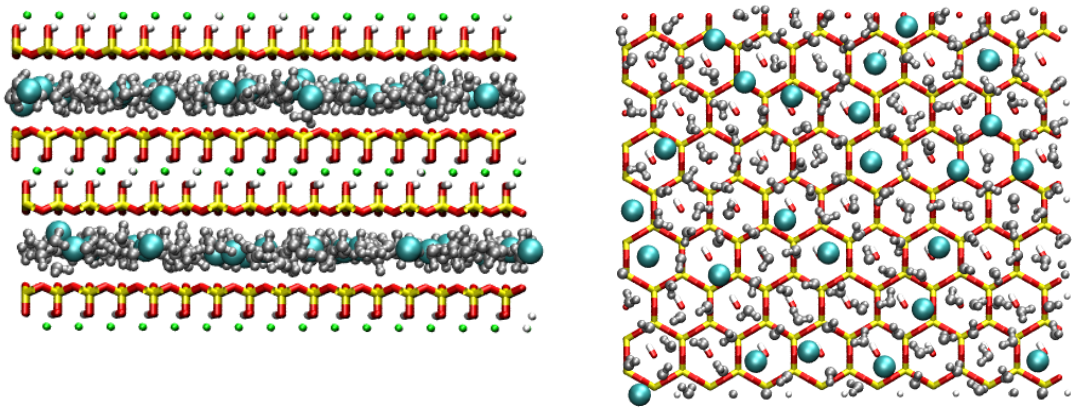

Figure 1. Cesium ions confined between montmorillonite clay surfaces. The interlayer porosity, seen from the side (left) and the top (right) also contains a monolayer of water. Cyan: Cs, yellow: Si, green: Al and Mg, red: O, white: H, grey: water molecules.

The motion of ions confined in these sub-nanometer pores has been studied extensively by molecular simulation [8–11]. It is almost two-dimensional and diffusive in the long time limit, with a linear growth of the mean-square displacement [12]. The corresponding diffusion coefficient

is ≈ 10 times smaller than in a bulk, infinitely diluted aqueous solution. In a previous work, we have investigated the possibility to describe this confined motion by a continuous solvent model in which the ion evolves in the Potential of Mean Force (PMF), which captures the average effect of all its environment (clay surfaces, water molecules and other ions). The effect of a thermalizing bath is then accounted for via a constant and uniform friction and random forces [5, 6]. The resulting model corresponds to simple Langevin Dynamics (for simplicity we write it here in the one-dimensional case):

$$\frac{\mathrm{d}v}{\mathrm{d}t} = \frac{F_{PMF}(t)}{m} - \gamma v(t) + \frac{R(t)}{m} \,, \tag{1}$$

where v is the velocity of the ion, m its mass, F_{PMF} the mean force acting on the ion at its current position, γ the friction and R a random force. The distribution of the latter is taken as Gaussian with a zero mean and a variance $\langle R(t)R(t')\rangle = 2\gamma m k_B T \delta(t-t')$, k_B being the Boltzmann constant, T the temperature and δ the Dirac distribution. In general, Lanvegin dynamics refers to numerical simulations based on the coupled stochastic equations for the evolution of N ions interacting via the instantaneous force due to the surfaces and to the other ions. In the following, however, we will use Langevin dynamics to refer to the effective one-body dynamics described by Eq. (1). Figure 2 compares the Velocity Autocorrelation Function (VACF) from Molecular Dynamics (MD) simulations with the results of Langevin dynamics in the PMF extracted from molecular simulations, for several values of the friction coefficient. It shows that no choice of friction allows to capture simultaneously the initial decay, the depth and the position of the minimum [5, 6].

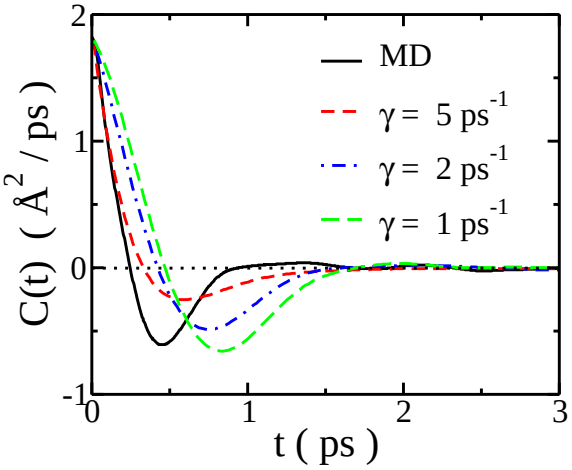

Figure 2. Velocity Autocorrelation Function (VACF) obtained by Molecular Dynamics (black curve) and by Langevin Dynamics using the potential of mean force extracted from molecular simulations, for different values of the friction γ (red, green and blue curves). None of these frictions is able to capture simultaneously the initial decay, the depth and the position of the minimum. Figure adapted from Ref. [6].

An underlying assumption of the Langevin equation (1) is the decoupling of time scales between the solute (ion) and its environment, which may not be achieved under extreme confinement conditions, despite the larger mass of the cesium ion compared to that of water molecules. The traditional way beyond this approximation is to describe the motion of the solute via a Generalized Langevin Equation (GLE), which in the absence of an external potential reads [13]:

$$\frac{\mathrm{d}v}{\mathrm{d}t} = -\int_0^t K(u)v(t-u)\,\mathrm{d}u + \frac{R(t)}{m} \,. \tag{2}$$

This equation introduces a memory kernel linked to the random force (noise) via the fluctuation-dissipation relation:

$$K(t) = \frac{\langle R(0)R(t)\rangle}{mk_BT} \tag{3}$$

Note that the simple Langevin equation corresponds to an infinitely fast relaxation of the noise, compared to the evolution of the velocity, *i.e.* $K(t) = 2\gamma\delta(t)$, with the friction coefficient:

$$\gamma = \int_0^\infty K(t)\mathrm{d}t. \tag{4}$$

In the limit of an infinitely heavy solute, this friction coefficient can be computed as the integral of the force autocorrelation function (FACF) instead of the memory kernel K [14, 15]. In the following, we discuss the extension of this framework to include the interactions with the confining surfaces. We first derive the relevant quantities to be determined using the Mori-Zwanzig formalism of projection operators. We then compute these quantities from molecular dynamics simulations. We finally discuss the applicability of such a strategy in the present case.

2.2 *Derivation of a Generalized Langevin Equation*

The Mori-Zwanzig formalism provides a natural route from the molecular Newtonian dynamics to coarse-grained models in which the dynamics is projected onto a reduced number of variables. We derive here a GLE for the evolution of the velocity of a solute under extreme confinement. In order to set the stage, let us first recall the standard derivation of Eq. (2) in the absence of such a potential. The starting point is the Liouville equation for the velocity of the solute:

$$\frac{\mathrm{d}v}{\mathrm{d}t} = i\mathcal{L}v \tag{5}$$

where the Liouvillian (super)operator $\mathcal{L}$ is related to the total Hamiltonian $\mathcal{H}$ of the system by: $i\mathcal{L} = \{H, .\}$. Since we aim at reducing the description of the whole system to the sole velocity v of an ion, we introduce the two operators P and Q defined by their action on any observable property $\mathcal{A}$ as:

$$\begin{aligned} P\mathcal{A}(t) &= \frac{\langle v(0)\mathcal{A}(t)\rangle}{\langle v(0)^2\rangle}v(0) = \frac{m\,\langle v(0)\mathcal{A}(t)\rangle}{k_BT}v(0) \\ Q\mathcal{A}(t) &= \mathcal{A}(t) - P\mathcal{A}(t)\ . \end{aligned} \tag{6}$$

The effect of P is to "project" the time-dependence of $\mathcal{A}$ on v, according to its correlation with the latter. Formal integration of the Liouville equation (5) allows to express the rate of change in the velocity from a given initial condition as:

$$\frac{\mathrm{d}v}{\mathrm{d}t} = e^{i\mathcal{L}t}i\mathcal{L}v(0) = e^{i\mathcal{L}t}\frac{F(0)}{m} + e^{i\mathcal{L}t}Q\frac{F(0)}{m}\ , \tag{7}$$

where we have introduced the fact that $P + Q = 1$ and $F(0) = m \times i\mathcal{L}v(0)$ the force acting on the solute arising from its interactions with the solvent. Using the parity properties of correlation functions, the hermitian properties of the Liouville operator and Dyson's relation [16], one obtains the GLE (2) with the memory kernel (3) and the explicit formal expression of the noise:

$$R(t) = e^{iQ\mathcal{L}t}F(0)\ . \tag{8}$$

We now turn to the more complex case where an external potential acts on the solute, and separate the total force as $F_{tot} = F_{ext} + F_{bath}$. Note that such a decomposition is very general and the choice of how to separate the force due to the external potential F_{ext} and to the thermal bath F_{bath} will be discussed below. Following the same procedure, we obtain the GLE:

$$\frac{\mathrm{d}v}{\mathrm{d}t} = \frac{F_{ext}(t)}{m} - \int_0^t v(t-u)K(u)\,\mathrm{d}u + \frac{R(t)}{m} \tag{9}$$

Despite a very strong ressemblance with Eq. (2), this result does not simply correspond to adding the external force to the equation of motion. Indeed, the memory K and noise R are now obtained by considering the action of the projection operators on the bath force only, instead of the total force, with the final result:

$$K(t) = \frac{\langle F_{tot}(0)R(t)\rangle}{mk_BT} \tag{10}$$

$$R(t) = e^{iQ\mathcal{L}t}F_{bath}(0)\ . \tag{11}$$

Note that the external potential is also present in the memory function K. Of course, in the absence of an external potential this reduces to the previous expressions.

Comparing the exact result of Eqs. (9-11) to the model of Ref. [6] described in the previous section, we now can explicit the approximations underlying the latter. On the one hand, it identifies the external force with the Potential of Mean Force $F_{PMF} = -\nabla\mathcal{V}_{PMF}$. This seems reasonable since the interaction with the clay indeed corresponds to an external potential, however the PMF also includes the average effect, for a given position of the solute, of the solvent and of the other solutes. On the other hand, it assumes that the remainder of the force $F_{bath} = F_{tot} - F_{PMF}$ relaxes very rapidly compared to the velocity of the solute so that its effect can be captured by a memory-less friction and a corresponding white noise. This assumption can be challenged by computing the memory kernel K from molecular simulations and comparing its relaxation with that of the VACF, as we now proceed to show. In addition, we analyze the effect of confinement on the separation of time scales between the solute and its environment by comparing the case of the cesium ion in the interlayer of montmorillonite and in bulk water. Finally, we discuss the contributions of the ion-clay, ion-water and ion-ion interactions to the total force and its relaxation.

3 Molecular simulations: methods

3.1 *System*

The simulated clay system, illustrated in Figure 1, contains two layers of montmorillonite (in the figure, one of these layers is divided into two halves shown on the top and bottom) of 8×4 unit cells each of unit cell formula $Cs_{0.75}Si_8(Al_{3.25}Mg_{0.75})O_{20}(OH)_4$. The 48 Cs^+ counterions, together with 288 water molecules, are located in the two interlayer porosities. The interlayer distance is 12.6 Å and the two layers are positioned so that the hexagonal cavities on their surface, visible in Figure 1, face each other. The lengths of the simulation box in the x and y directions parallel to the clay layers are 41.44×35.88 Å^2. For the aqueous Cs^+ ion, the cubic box of length 18.65 Å contains 1 ion and 215 water molecules. Periodic boundary conditions are applied in all directions.

The water molecules are described according to the SPC/E force field [17], the cesium ions by the force field from Koneshan *et al.* [18], and the clayFF force field is used for the clay layers [19]. The latter are considered rigid and the corresponding atomic positions are set to the experimental data [20]. Long-range electrostatic interactions are computed using Ewald summation [21]. Molecular dynamics in the NVT-ensemble are performed using a Nosé-Hoover

thermostat with a time constant of 0.5 ps. The system is first randomized at 1000 K for 10 ps, then equilibrated at 298 K for 80 ps. The properties are subsequently determined in NVE runs with different lengths: 10 simulations of 35 ps and 4 simulations of 5 ns for the short and long time dynamics, respectively. Newton's equation of motion are solved using the Leap-Frog Verlet algorithm with a time-step of 1 fs. All simulations were performed using the DL_POLY simulation package [22].

3.2 *Potential of Mean Force*

The two-dimensional PMF is computed from the equilibrium one-body density as: $\mathcal{V}_{PMF}(x,y) = -k_BT \ln \rho(x,y)$. The latter is determined by averaging over ten trajectories of 35 ps, over the 48 ions and exploiting the hexagonal symmetry of the cavities on the surface. Since the mean force needs to be evaluated at any position in order to extract the bath force, we further use an analytical approximation to represent it using the following expression, which corresponds to the above-mentioned symmetry of the unit-cell:

$$\begin{aligned}\mathcal{V}_{PMF}^{analy}(x,y) = -k_BT \sum_{n_x=0}^{6}\sum_{n_y=0}^{6} A(n_x,n_y) \Bigg[&\cos\left(\frac{4\pi n_x x}{a_x}\right)\cos\left(\frac{4\pi n_y y}{a_y}\right) \\ &+ \cos\left(\frac{2\pi n_x (x+y\sqrt{3})}{a_x}\right)\cos\left(\frac{2\pi n_y (y-x\sqrt{3})}{a_y}\right) \\ &+ \cos\left(\frac{2\pi n_x (x-y\sqrt{3})}{a_x}\right)\cos\left(\frac{2\pi n_y (y+x\sqrt{3})}{a_y}\right)\Bigg] ,\end{aligned} \tag{12}$$

with a_x and a_y the dimensions of the unit cell. The coefficients $A(n_x,n_y)$ are determined numerically so as provide the best fit to the molecular simulation results, using the MINUIT software [23]. The mean force F_{PMF} is then computed at each time step as the derivative of this expression, evaluated at the position of the cesium ion.

3.3 *Computation of the noise and of the memory kernel*

While the extraction of the VACF and FACF from a MD trajectory is straightforward, as the velocity and force acting on each particles are readily available, the determination of the noise R, hence of the memory kernel K, is much more involved. Indeed, the projected forces do not evolve simply according to the Liouvillian as in Eq. (5), but according to the projected operator $iQ\mathcal{L}$. By differentiating the definition Eq. (11) with respect to time and using the properties of the projector Q, we obtain the following evolution equation for the noise [24]:

$$\frac{\mathrm{d}R}{\mathrm{d}t} = i\mathcal{L}R(t) + \frac{\langle F_{tot}(0)R(t)\rangle}{k_BT} v \tag{13}$$

which has to be solved for the initial condition:

$$R(0) = F_{bath}(0) \ . \tag{14}$$

The numerical algorithm allowing to reconstruct *a posteriori* the noise from a MD trajectory will be presented in Ref. [25], which discusses two algorithms based on different points of view (looking forward or backward in time) and illustrates their relative merits on the case of a Lennard-Jones fluid. For each configuration of the trajectory, the bath force is determined by

substracting the analytical representation of the mean force from the total force and used as the initial condition to integrate Eq. (13). The memory kernel is finally obtained from its definition Eq. (10).

3.4 *Force Splitting*

In order to assess the relative contributions to the overall force on the confined ion due to the ion-clay (C), ion-water (W) and ion-ion (I) interactions, these forces must be computed separately at each time step of the trajectory. The timescales on which they evolve and their possible coupling can then be quantified by their auto- and cross-correlation functions.

4 Results and Discussion

4.1 *Potential of Mean Force*

The two-dimensional PMF for a Cs^+ ion in a monohydrated montmorillonite is reported in Figure 3. It displays a global minimum corresponding to the ion above the center of the hexagonal cavity as well as secondary minima above the surface silicon atoms (*i.e.* coordinated by three surface oxygen atoms to which the silicon is bonded). Both situations can be observed on Figure 1. The diffusion of the Cs^+ ion from one cavity to another involves hopping through the secondary minima, with an activation barrier of $\sim 3k_BT$. These results are in qualitative agreement with those of Ref. [5, 6] obtained with a different force field.

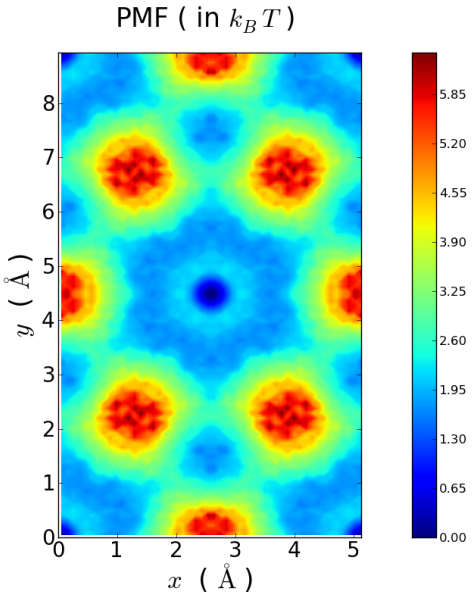

Figure 3. Two-dimensional Potential of Mean Force (PMF) in units of the thermal energy k_BT for an interlayer cesium ion.

4.2 *Short time dynamics*

The main purpose of the present paper is to assess the relevance of a continuous solvent model to describe the dynamics of ions confined down to the molecular scale. The VACF for Cs^+ confined in the interlayer of montmorillonite in the monolayer hydration state is reported in Figure 4. In agreement with previous simulations of the same system using a different force field [5], we find that the VACF decreases from k_BT/m to a negative minimum value ($\approx -0.25k_BT/m$) in

approximately 0.5 ps, before decaying to 0 for $t \approx 1$ ps). As mentioned above, the simple Langevin equation (1) has been shown to fail to reproduce this VACF obtained by molecular simulation [5, 6]. We now investigate in more detail the validity of the main approximation underlying this model, namely that the thermal bath which models the deviation of the instantaneous force from the mean force, evolves on a faster time scale than the solute.

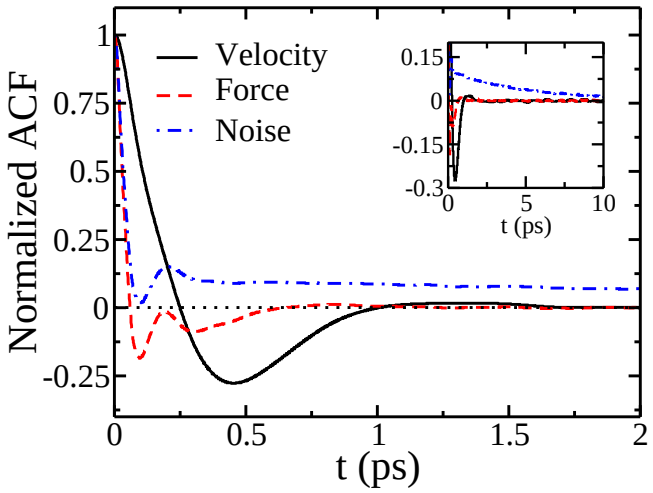

Figure 4. Normalized autocorrelation functions for the velocity (VACF), force (FACF) and noise (memory function K), for an interlayer cesium ion. The insert shows the slower decay of the memory function compared to the VACF and FACF.

In the limit of an infinitely heavy solute (compared to the solvent) the friction coefficient of the Langevin equation (1) is given by the integral of the force autocorrelation function (FACF) [14, 15]. Such an assumption may seem reasonable in the case of the Cs^+ which is ≈10 times heavier than a water molecule. The FACF, also reported in Figure 4 decays to zero more rapidly than the VACF, within 0.5 ps, after a significantly faster initial decrease (0.1 ps) to a negative minimum ($\approx -0.2 \left\langle \mathbf{F}^2 \right\rangle$) followed by a shallower one ($\approx -0.1 \left\langle \mathbf{F}^2 \right\rangle$ at 0.3 ps). Under the above approximation, the relatively fast decorrelation of the force compared to the velocity, even though not complete, may suggest that the Brownian approximation is reasonable.

However, the relevant correlation function to define the memory kernel K is the noise autocorrelation function (NACF), as can be seen in Eq. (10). The NACF, computed from the noise extracted from the trajectory as explained in Section 3.3, is reported for the confined ion in Figure 4. It coincides with the FACF at very short times (up to 50 fs) and its variations up to 250 fs, with a miminum followed by a maximum, clearly ressemble that of the FACF in this intermediate regime. Nevertheless, there are significant differences between the memory kernel and the FACF. Firstly, contrary to the latter, the memory is always positive. Secondly, and most strinkingly, the memory appears to level off at a plateau, at ≈ 10% of its initial value after 400 fs. It then decays to zero on a much longer time scale, larger than 10 ps (see insert of Figure 4). This slow decay of the memory kernel compared to the VACF, which constitutes the main result of the present work, pinpoints the failure of the simple Langevin model, as the latter assumes an instantaneous relaxation of the solute-bath interaction compared to the dynamics of the solute (VACF). It may seem that the fast initial decay, which decreases the memory kernel by an order of magnitude, is sufficient to ensure a separation of time scales and the proper definition of a friction coefficient. This is however not the case, as the slower decay from this smaller value contributes significantly to the integral of K, which would define the friction if such a concept were applicable.

4.3 *Confined vs bulk ions*

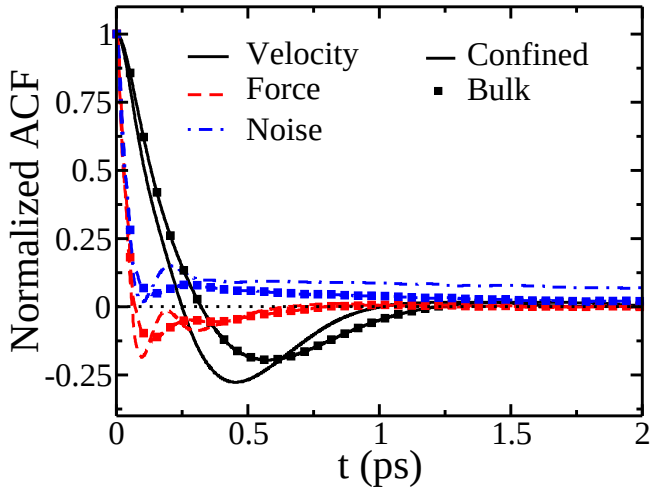

Figure 5. Normalized autocorrelation functions for the velocity (VACF), force (FACF) and noise (memory function K): comparison between a cesium ion in the interlayer of montomorillonite clay (lines without symbols) and in bulk water (lines with symbols).

Before analyzing in more detail the microscopic origin of this slow decay of the memory kernel, let us first compare the dynamics of confined Cs^+ with that in bulk water. Figure 5 compares the normalized VACF, FACF and memory kernel in the bulk and confined cases. The bulk results for the VACF and FACF are qualitatively similar to the confined case, even though quantitative differences are observed. For example, the decay of the VACF is slightly slower in the bulk and the negative minimum is only $\approx -0.2 k_B T/m$. The initial decay of the FACF is almost identical to the confined case, but the subsequent oscillations are less pronounced. The impact of confinement is the largest on the memory kernel, which is the most important of the three correlation functions for the purpose of deriving continuous solvent models. The memory kernel, which follows the same initial sharp decay in the bulk and under extreme confinement, does not exhibit a plateau on this time scale and decays much more rapidly than in the confined case. Note that even in this case the contribution of the power-law decay (not visible on the figure) of the memory kernel to the integral which defines the friction coefficient is non negligible. In the bulk, this corresponds to the hydrodynamic backflow of solvent, which occurs on a time scale longer than the typical collision time with the solute with its neighbouring solvent molecules reflected in a negative minimum of the VACF for ≈ 0.5 ps.

4.4 *Ion-water, ion-surface and ion-ion interactions*

The sharper decay and oscillations of the VACF under extreme confinement suggests that the interaction of Cs^+ with water molecules is more repulsive in that case. The confined water molecules cannot transfer momentum to the rest of the fluid as easily as in the bulk and the solvent cage around the ion is stronger. In addition, the slower decay of the memory kernel also reflects the hindered momentum transfer to the rest of the fluid. In order to further quantify the role of ion-clay (IC), ion-water (IW) and ion-ion (II) interactions on the dynamics of the confined ion, we now analyze their correlation functions. Figure 6 reports the auto- and cross-correlation functions for these three specific forces, along and perpendicular to the clay surfaces.

In the direction along the surface, all these correlation functions do not show any significant variation over the picosecond time scale, with the notable exception of the ion-water autocorrelation function, which displays a minimum for $\approx$0.1 ps followed by a plateau. This clearly

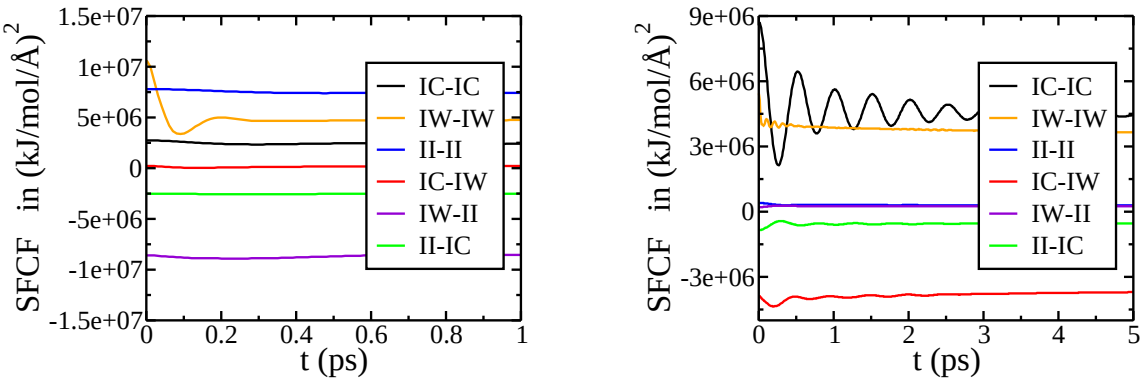

Figure 6. Specific force correlation functions (SFCF), for the three contributions to the force acting on the ion: ion-clay (IC), ion-water (IW) and ion-ion (II) interactions. Both auto- (IC-IC, IW-IW, II-II) and cross- (IC-IW, IW-II, II-IC) correlation functions are reported. **Left** Components parallel to the surface. **Right** Component perpendicular to the surface.

demonstrates that the evolution of the FACF and of the memory kernel discussed in the previous section is due to the ion-water interactions and more precisely to the oscillations of the Cs^+ ion in a solvent cage which otherwise does not evolve on this time scale. One can futher notice that the order of magnitude of all forces is similar: The initial value of the *auto*-correlation functions increases by a factor of 4 from ion-clay to ion-ion and ion-water interactions (IC-IC, II-II and IW-IW on Figure 6, respectively), indicating a two-fold increase in $\sqrt{\langle \mathbf{F}^2 \rangle}$. In addition, the ion-clay and ion-water interactions are almost uncorrelated (small values of the *cross*-correlation function) , while the ion-ion interactions are anti-correlated with both the ion-water and ion-clay interactions (negative *cross*-correlation functions). Since the environment of the ion is frozen on this time scale, the ion-ion interaction and the parallel component of the ion-clay interaction can be considered constant and the anti-correlation only reflects the fact that the total force vanishes on average.

The force experienced by the confined ion in the direction perpendicular to the surfaces is, as expected, dominated by the ion-clay interaction, since the vertical confinement results from the steric repulsion by the clay surface. The perpendicular component of ion-ion interaction is negligible compared to the ion-clay and ion-water interactions, because the ion-ion vectors are approximately parallel to the surfaces. In that direction, only the ion-clay interaction evolves significantly over a few ps as the ion oscillates on this time scale, as indicated by the weakly damped oscillatory behaviour of the perpendicular component of this force. Note that it does not decay to zero on this time scale, reflecting the asymmetry of the instantaneous local environment of the ion near the middle of the interlayer. Thus the description of the system as purely two-dimensional is only approximate. As for the parallel component, the anti-correlation between the ion-clay and ion-water interactions reflects the vanishing of the total force on average over this time scale.

4.5 *Long-time dynamics*

All these correlation functions decay to zero on a much longer time scale, as illustrated on Figure 7. Despite the decorrelation of the total force within 1 ps, it takes several ns for the ion-water, ion-clay and ion-ion interactions to decorrelate. The picture that emerges from this observation, together with the previous results, is that of a multi-scale process, with a short equilibration of the ion inside a local free energy minimum corresponding to a surface cavity and a solvent cage, and a much slower relaxation of this local environment and the corresponding motion of the ion to another local free energy minimum. Such slow relaxation is reminiscent of that observed in glasses or with site-to-site hopping in solids. The theoretical tools used to

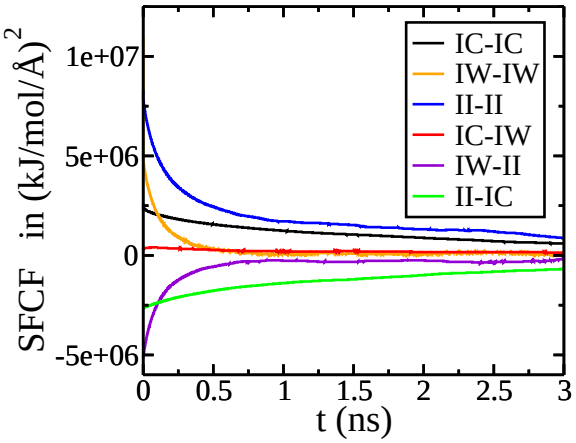

Figure 7. Correlation functions of the different forces acting on the ion. The total force is separated into ion-clay (IC), ion-water (IW) and ion-ion (II) interactions. Both auto- (IC-IC, IW-IW, II-II) and cross- (IC-IW, IW-II, II-IC) correlation functions are reported, for the components parallel to the surfaces.

model the dynamics of such systems may thus prove useful in the description of the long-time dynamics of solutes under extreme confinement.

5 Conclusion

Using the Mori-Zwanzig formalism of projection operators, we have derived a Generalized Langevin Equation for the continuous solvent description of the dynamics of a confined solute. The solute evolves in the Potential of Mean Force under the effect of a random noise and a friction with a memory that both differ from that in a bulk solvent. As an example, we have considered the case of the Cs^+ ion confined in the interlayer of montmorillonite clays with a very low water content. We have computed the memory kernel from molecular dynamics simulations and have shown that it decays on a time scale longer that 10 ps, while the main features of the velocity autocorrelation function decay within a few ps. Thus there is no separation of time scales between the dynamics of the confined Cs^+ and that of the confined solvent, despite the much larger mass of the ion. This explains why the dynamics of this ion under extreme confinement cannot be described by a simple Langevin equation, as was previously attempted.

In the bulk, the slowest decay mode for the memory function, which is faster than in the confined case, corresponds to the hydrodynamic backflow of the solvent, while the shortest corresponds to the collision of the solute with its solvent cage. In order to understand the microscopic origin of the slow decay of the memory function under extreme confinement, we have further analyzed the relative contribution of the ion-surface, ion-solvent and ion-ion interactions to the dynamics. On the ps time scale, the only appreciable motion corresponds to the vibration of the ion in its neighbour cage, which involves the clay atoms in the direction perpendicular to the surface and water molecules in the direction parallel to the surfaces. This cage relaxes on a much longer (up to several ns) time scale, with the hopping of ions between local free energy minima, probably via the correlated motion of ions and solvent molecules. The resulting overall dynamics ressembles that of glasses or diffusion inside a solid by site-to-site hopping. This work opens a new perspective for the description of the dynamics of ions in water under extreme confinement, which could be applied in other materials of great scientific and practical relevance, such as zeolites [26] or carbon nanotubes [27]. Since in the bulk a Langevin description is relevant, it would be interesting to investigate wider pores, such as silica slit pores with a few water layers [28], in order to determine where the cross-over between the extreme confinement and bulk-like regimes takes place.

Acknowledgements

The authors thank Rodolphe Vuilleumier and Jean-François Dufrêche for useful discussions. AC acknowledges financial support from the Ecole Normale Supérieure (Paris). VM, MS, JPH, PT and BR acknowledge financial support from the Agence Nationale de la Recherche under grant ANR-09-SYSC-012.

References

[1] L. Bocquet and J.L. Barrat, *Hydrodynamic properties of confined fluids*, Journal of Physics: Condensed Matter 8 (1996), p. 9297.
[2] L. Bocquet and J.L. Barrat, *Flow boundary conditions from nano-to micro-scales*, Soft Matter 3 (2007), pp. 685–693.
[3] L. Bocquet, *High friction limit of the Kramers equation: The multiple time-scale approach*, American Journal of Physics 65 (1997), p. 140.
[4] L. Bocquet, *From a stochastic to a microscopic approach to Brownian motion*, ACTA PHYSICA POLONICA SERIES B 29 (1998), pp. 1551–1564.
[5] B. Rotenberg, V. Marry, J.F. Dufrêche, E. Giffaut, and P. Turq, *A multiscale approach to ion diffusion in clays: Building a two-state diffusion-reaction scheme from microscopic dynamics*, Journal of Colloid and Interface Science 309 (2007), pp. 289–295.
[6] J.F. Dufrêche, B. Rotenberg, V. Marry, and P. Turq, *Bridging molecular and continuous descriptions: the case of dynamics in clays*, Anais da Academia Brasileira de Ciencias 82 (2010), pp. 61–68.
[7] M.A. Glaus, B. Baeyens, M.H. Bradbury, A. Jakob, L.R. Van Loon, and A. Yaroshchuk, *Diffusion of ^{22} Na and ^{85} Sr in Montmorillonite: Evidence of Interlayer Diffusion Being the Dominant Pathway at High Compaction*, Environmental Science & Technology 41 (2007), pp. 478–485.
[8] V. Marry, P. Turq, T. Cartailler, and D. Levesque, *Microscopic simulation of structure and dynamics of water and counterions in a monohydrated montmorillonite*, The Journal of Chemical Physics 117 (2002), p. 3454.
[9] V. Marry and P. Turq, *Microscopic Simulations of Interlayer Structure and Dynamics in Bihydrated Heteroionic Montmorillonites*, The Journal of Physical Chemistry B 107 (2003), pp. 1832–1839.
[10] N. Malikova, V. Marry, J.F. Dufrêche, and P. Turq, *Na/Cs montmorillonite: temperature activation of diffusion by simulation*, Current Opinion in Colloid & Interface Science 9 (2004), pp. 124–127.
[11] N. Malikova, A. Cadène, V. Marry, E. Dubois, and P. Turq, *Diffusion of Water in Clays on the Microscopic Scale: Modeling and Experiment*, The Journal of Physical Chemistry B 110 (2006), pp. 3206–3214.
[12] V. Marry, N. Malikova, A. Cadene, E. Dubois, S. Durand-Vidal, P. Turq, J. Breu, S. Longeville, and J.M. Zanotti, *Water diffusion in a synthetic hectorite by neutron scattering beyond the isotropic translational model*, Journal of Physics: Condensed Matter 20 (2008), p. 104205.
[13] J.P. Hansen and I.R. McDonald, *Theory of Simple Liquids, Third Edition* 3rd ed., Academic Press, 2006.
[14] P. Mazur and I. Oppenheim, *Molecular theory of Brownian motion*, Physica 50 (1970), pp. 241–258.
[15] P. Espanol and I. Zuniga, *Force autocorrelation function in Brownian motion theory*, The Journal of Chemical Physics 98 (1993), pp. 574–580.
[16] R. Zwanzig, *Nonequilibrium Statistical Mechanics* 1st ed., Oxford university Press, 2001.
[17] H.J.C. Berendsen, J.R. Grigera, and T.P. Straatsma, *The missing term in effective pair potentials*, Journal of Physical Chemistry 91 (1987), pp. 6269–6271.
[18] S. Koneshan, J.C. Rasaiah, R.M. Lynden-Bell, and S.H. Lee, *Solvent Structure, Dynamics, and Ion Mobility in Aqueous Solutions at 25 C*, The Journal of Physical Chemistry B 102 (1998), pp. 4193–4204.
[19] R.T. Cygan, J.J. Liang, and A.G. Kalinichev, *Molecular Models of Hydroxide, Oxyhydroxide, and Clay Phases and the Development of a General Force Field*, The Journal of Physical Chemistry B 108 (2004), pp. 1255–1266.
[20] E. Maegdefrau and U. Hoffman, *Die Kristallstruktur des Montmorillonits*, Z. Kristallogr. Kristallgeom. Kristallphys. Kristallchem. 98 (1937), pp. 299–323.
[21] D. Frenkel and B. Smit, *Understanding Molecular Simulations, From Algorithms to Applications* Academic Press, 2002.
[22] W. Smith and T. Forester, *DLPOLY2 user manual* Daresbury Laboratory, 2001.
[23] F. James and M. Roos, *MINUIT - System for function minimization and analysis of parameter errors and correlations*, Comp. Phys. Commun. 10 (1975), pp. 343–367.
[24] E. Darve, J. Solomon, and A. Kia, *Computing generalized Langevin equations and generalized Fokker-Planck equations*, Proceedings of the National Academy of Sciences 106 (2009), pp. 10884–10889.
[25] A. Carof, R. Vuilleumier, and B. Rotenberg, In preparation; .
[26] M. Jeffroy, A. Boutin, and A.H. Fuchs, *Understanding the Equilibrium Ion Exchange Properties in Faujasite Zeolite from Monte Carlo Simulations*, The Journal of Physical Chemistry B 115 (2011), pp. 15059–15066.
[27] D.J. Bonthuis, K.F. Rinne, K. Falk, C.N. Kaplan, D. Horinek, A.N. Berker, L. Bocquet, and R.R. Netz, *Theory and simulations of water flow through carbon nanotubes: prospects and pitfalls*, Journal of Physics: Condensed Matter 23 (2011), p. 184110.
[28] D. Argyris, D.R. Cole, and A. Striolo, *Ion-Specific Effects under Confinement: The Role of Interfacial Water*, ACS Nano 4 (2010), pp. 2035–2042.